University of Trento

Department of Physics

Bachelor's Degree in Physics

Chaotic Dynamics in the Burridge-Knopoff Model of Earthquake Faults

Supervisor
Prof. Leonardo Ricci

Co-supervisor
Dr. Alessio Perinelli

Author
Sebastiano Guaraldo
matr. 213380

Academic year 2021-2022

Ai miei genitori
che mi hanno sempre dato fiducia, supportato nelle mie scelte e che,
soprattutto, mi vogliono bene.

Contents

Chapter 1

Introduction

On August 2nd in 2027 there will be a total solar eclipse visible (at least partially) from South/West Europe, South/West Asia, much of Africa, Atlantic and Indian Ocean. The full eclipse will begin at 8:23:20 UTC and will end at 11:49:48 UTC; its maximum phase will be at 10:06:36[1]. We are able to predict eclipses because the motion of planets and satellites (neglecting small relativistic corrections) is governed by classical mechanics which is deterministic. If the forces acting on a body are known, given its initial position and speed, the laws of Newtonian mechanics allow us to calculate, with great precision, the future trajectory.

At the end of the XIX century some theoretical physicists like Ludwig Boltzmann started to put in doubt the concept of absolute determinism, introducing statistics and probability to give a mechanical interpretation of thermodynamics. These ideas are the basis of statistical mechanics that connects thermodynamic quantities (such as pressure, temperature, heat capacity...) to microscopic behaviour of particles. The macroscopic properties of a body do not depend on the detail movements of its molecules but on statistical averages evaluated on a large number of molecules. In this sense probability has become part of mechanics, despite the fact that the microscopic motions of the particles are in any case deterministic.

Quantum mechanics, and in particular Heisenberg's uncertainty principle, brought a deeper revision of the idea of determinism. According to the theory we can't predict with absolute certainty the position of a particle but we can only evaluate the probability to find it in a specific point of the space. The trajectory in quantum mechanics is indeed an idea which has no sense. However when we consider systems where the results of quantum mechanics are negligible (e.g. macroscopic systems) the predictions given by classical mechanics are correct.

Nevertheless there exist deterministic systems, governed by well determined laws, that behave in an irregular and apparently random way. We talk of *chaotic systems*. The characteristics of these systems are different from those of a purely random system. One of the most important of these features is the sensitivity to initial conditions: even if the state of a system is determined in a deterministic way, small differences in the initial conditions (such as those due to errors

[1] https://www.timeanddate.com/eclipse/solar/2027-august-2

in measurements or due to rounding errors in numerical computation) can produce effects exponentially different in final states, making long-term predictions extremely difficult and unreliable. While it is typically true that “small initial variations produce small final effects”, this is no longer valid for chaotic systems. This fact is well summarized by the words of the American mathematician and meteorologist Edward Lorenz:

> “Chaos: When the present determines the future, but the approximate present does not approximately determine the future.”

The strong dependence on the initial state is well known also with the name of *butterfly effect*, a term coined by Lorenz in the meteorological field and nowadays also used outside the mathematical sciences.

In addition to the sensitivity to initial conditions, deterministic chaotic systems exhibit other interesting properties, such as recurrence, irregular and aperiodic dynamics, non-linearity, self-similarity and fractality. These will be discussed in the next chapters.

In order for a system to have chaotic behavior it does not need to be described by complex equations and to depend on a large number of variables. In the case of systems whose evolution depends continuously on time, only three variables are sufficient for chaos to be possible. This allows to demonstrate and study the essential characteristics of chaos in relatively simple systems, such as a pendulum. This important achievement of the theory of chaos has brought to numerous studies in various disciplines besides mathematics and physics. Biology, chemistry, computer science, economics, sociology and even anthropology have found the tools to study their systems in the mathematics of chaos. The fact that simple equations can have solutions of incredible complexity continues to fascinate scientists and raises the hope that phenomena previously thought too complicated to be understood might be adequately described by very simple models.

From what has been said so far, it is clear that chaos is a dynamical regime with unique characteristics and it is particularly interesting because it could be at the origin of phenomena that seem random, or at least irregular, but which could instead have an underlying deterministic dynamics. Chaos theory would therefore provide a better understanding of systems that have hitherto been considered completely stochastic, and then unpredictable in their behaviour, but which could exhibit chaotic dynamics. One such system is the *lithosphere*, and earthquakes in particular.

Earthquakes are indeed extremely complex phenomena and, nowadays, impossible to predict accurately. This inability to make long-term predictions may depend on many factors, and it is evident how important it is to build models that can help to understand the dynamics behind these catastrophic events. In particular, it is interesting to see whether there may be chaos in some earthquake models.

The purpose of this thesis is to analyze a relatively simple[2] model, called *Burridge-Knopoff model*, introduced to study nonlinear effects arising in the dynamics of earthquake faults. So far, a large number of different models and algorithms have been developed to calculate earthquake forecasts. In this work, the main goal is to reproduce and discuss the results obtained by de Sousa Vieira [1] by trying to go into more detail about the problem and in order to lay the foundations for possible future research. In fact, there are not many studies on the subject, despite the importance that a possible discovery in this area could have both in terms of understanding the dynamics of the Earth's crust (in particular, from a physical point of view, with regard to the presence of chaotic behaviour) and in predicting seismic events. Chaos is in indeed difficult to detect in complex systems which are impossible to reproduce in laboratories, as instead happens with electrical circuits that are easily controlled and set. For this reason, solid evidence of its presence in the lithosphere could be significant.

The present thesis is organized as follows. The basic concepts of chaos theory are presented in Chapter 2 while in Chapter 3 we will introduce the Burridge-Knopoff (BK) model, numerically simulate the symmetric two-block system and shortly talk about the three-block model. The results obtained will then be discussed and we will draw conclusions in Chapter 4.

[2]Despite being a simple model, it still capable of giving rise to dynamics that show the same features as seismic events.

Chapter 2

Dynamical Systems and Chaos

Typically, in the various branches of science, we are interested in the study of *dynamical systems*, whose state changes in time. These systems, whether natural or artificial, exhibit a wide variety of dynamical regimes: there may be stable fixed points, periodic and regular evolutions, aperiodic or stochastic trends. Particularly interesting are the *chaotic dynamical regimes*, characterized by aperiodicity, irregularity and unpredictability (similar to random processes) despite being ruled by deterministic laws. This chapter will describe the fundamental concepts of *dynamical* and in particular *chaotic* systems.

2.1 An Historical Overview of Chaos

Before examining dynamical systems theory and chaos theory in detail, let's see how the idea that a physical system can exhibit chaotic behaviour came about. In Chapter 1, some properties of chaotic dynamics have already been mentioned. We spoke in particular of sensitivity to initial conditions by introducing the famous *butterfly effect*. This expression comes from the lecture E. Lorenz gave on December 1972 at a session of the annual meeting of the AAAS (American Association for the Advancement of Science) entitled "Predictability: Does the Flap of a Butterfly's Wings in Brazil Set Off a Tornado in Texas?" [2]. The question which really interested the author was whether, for example, two particular weather situations differing by as little as the immediate influence of a single butterfly will generally after sufficient time evolve into two situations differing by as much as the presence of a tornado. In more technical language, is the behavior of the atmosphere unstable with respect to perturbations of small amplitude? Actually, Henri Poincarè had already developed similar ideas about this sensitivity to initial conditions, almost in the same terms, in his work *Science and method* [3]:

> "Why have meteorologists such difficulty in predicting the weather with any certainty? Why is it that showers and even storms seem to come by chance, so that many people think it quite natural to pray for rain or fine weather, though they would consider it ridiculous to

> ask for an eclipse by prayer? We see that great disturbances are generally produced in regions where the atmosphere is in unstable equilibrium. The meteorologists see very well that the equilibrium is unstable, that a cyclone will be formed somewhere, but exactly where they are not in a position to say; a tenth of a degree more or less at any given point, and the cyclone will burst here and not there, and extend its ravages over districts it would otherwise have spared. If they had been aware of this tenth of a degree, they could have known it beforehand, but the observations were neither sufficiently comprehensive nor sufficiently precise, and that is the reason why it all seems due to the intervention of chance. Here, again, we find the same contrast between a very trifling cause that is inappreciable to the observer, and considerable effects, that are sometimes terrible disasters."

Indeed, an early proponent of chaos theory was Henri Poincaré himself. At the end of the XIX century, while studying the problem of the motion of three celestial bodies experiencing mutual gravitation attraction, he found that there can be orbits that are nonperiodic, and yet not forever increasing nor approaching a fixed point [4]. Others subsequently devoted themselves to the study of these chaotic dynamics, for example G. Birkhoff in the 1920s or M. L. Cartwright and J. E. Littlewood in the 1940s. In spite of this work, however, the possibility of chaos in real physical systems was not widely appreciated until relatively recently. The reasons for this were that first of all the mathematical papers were difficult to read for workers in other fields, and secondly that the proven theorems often failed to convince researchers in these other fields that this type of behaviour would have been important in their systems. The situation has now changed thanks to computers that allow to obtain numerical solutions of dynamical systems. Using such solutions the chaotic character of the time evolutions in situations of practical importance has become clear.

Edward Lorenz was a pioneer of the theory but he actually got in touch with chaos accidentally while studying the atmosphere and working on weather prediction. Lorenz developed a simplified mathematical model of the air moving in the atmosphere and used a simple digital computer to run his weather simulation. As he wrote in one of his book [5], he wanted to repeat some of the computations in order to examine what was happening in greater detail. He stopped the computer, typed in a line of numbers that it had printed out a while earlier, and set it running again. To his surprise, the weather the machine began to predict was completely different from the previous calculation. The problem was that the computer worked with 6-digit precision, but the printout rounded variables off to a 3-digit number. The difference is tiny, and the consensus at the time would have been that it should have no practical effect. However, Lorenz discovered that small changes in initial conditions produced large changes in long-term outcome. In his famous paper "Deterministic nonperiodic flow" [6], in fact, he described a relatively simple system of equations that resulted in an infinite series of extremely complex solutions that showed a sensitive dependence on the initial data. In today's terminology, there was chaos.

2.2 Dynamical Systems

A dyamical system is one whose state changes in time. If these changes are driven by specific rules, we say that the system is *deterministic*; otherwise, if the rules are random, it is *stochastic*. This thesis will be concerned with deterministic dynamical systems.

Mathematically, a dynamical system may be defined as a collection of deterministic mathematical laws that describe the evolution in time of the state of a system. In this framework, time can be either a discrete or continuous variable and consequently we can speak of discrete or continuous dynamical system. An example of the latter is a system of N first-order autonomous, ordinary differential equations which can be written, in vector form, as:

$$\frac{\mathrm{d}\mathbf{x}(t)}{\mathrm{d}t} = \mathbf{F}[\mathbf{x}(t)] \tag{2.1}$$

where $\mathbf{x}(t)$ is an N-dimensional vector. This system is deterministic because in principle, for any given initial state $\mathbf{x}(0)$, we can solve the equations to obtain the future state $\mathbf{x}(t)$ for $t > 0$. The system is also called autonomous because the function $\mathbf{F}[\mathbf{x}(t)]$ does not explicitly depend on time (which is the independent variable). The space $\mathcal{S} \subseteq \mathbb{R}^N$ of the all possible states $\mathbf{x}(t)$ of the system is referred to as *state space*. For mechanical systems, the phase space typically consists of all possible values of position and momentum variables and it is usually called *phase space*. Evolving with time, the system follows a path in this space which is called *trajectory* or *orbit*. The simultaneous motion of all the points in the state space (considered as initial conditions) looks like a flowing fluid and hence systems such as (2.1) are typically called *flows*.

In the case of discrete time variable, a dynamical system is defined iteratively by a map:

$$\mathbf{x}_{n+1} = \mathbf{M}(\mathbf{x}_n) \tag{2.2}$$

where $\mathbf{x}_n$ is the state of the system at the time t_n. If we have always the same time step τ then $t_n = n\tau$. As a result of this description, we are able to generate an orbit of the discrete system (that will be a succession such as $\mathbf{x}_0, \mathbf{x}_1, \mathbf{x}_2, ...$) given an initial condition $\mathbf{x}_0$.

2.3 Attractors

In Hamiltonian systems (according to Liouville's theorem) there exists choices of the phase space variables (e.g. the canonically conjugate position and momentum variables) for which the phase space volumes are preserved under time evolution [7]. Thus, given at the initial time $t = 0$ a closed $(N-1)$-dimensional surface S_0 in the phase space (which is N-dimensional), each point on the surface can be evolved forward in time using itself as initial condition in (2.1) and in this way S_0 evolves to a closed surface S_t at some later time t. As stated above then the N-dimensional volumes V_0 of the portion of the phase space enclosed by S_0 and V_t, of the region enclosed by S_t, are the same. Systems that satisfy this condition are called *conservative* since they conserve energy but they are rare in nature. For these systems the flow is also time-reversible [8].

An example of conservative system is the pendulum described by the equations (mass, length and gravitational acceleration are assumed to be unitary):

$$\begin{aligned} \frac{\mathrm{d}x}{\mathrm{d}t} &= v \\ \frac{\mathrm{d}v}{\mathrm{d}t} &= -\sin(x) \end{aligned} \tag{2.3}$$

where x is the angle (in radians) that the pendulum makes from the vertical and v is the angular velocity.

On the other hand if the flow, even with a change of variables, does not preserves volumes then the system is said to be *non-conservative* and in particular if there is volume contraction we speak of *dissipative* systems. We have, by the divergence theorem, that:

$$\frac{\mathrm{d}V(t)}{\mathrm{d}t} = \int_{S_t} \nabla \cdot \mathbf{F}\, d^N x \tag{2.4}$$

where the integral is over the volume interior to the surface S_t. If there exists a region of phase space where $\nabla \cdot \mathbf{F} < 0$ then there we have a dissipative system which do not conserve mechanical energy and are not time-reversible [8]. These systems are typically characterized by the presence of bounded subsets in the phase space to which regions of initial conditions (of nonzero phase space volume) evolve as time increases called *attractors*.

For instance, it is more realistic for the pendulum to consider a friction term due mainly to air resistance and assumed to be proportional to the magnitude of the velocity and directed opposite to it. The equations (2.3) become:

$$\begin{aligned} \frac{\mathrm{d}x}{\mathrm{d}t} &= v \\ \frac{\mathrm{d}v}{\mathrm{d}t} &= -bv - \sin(x) \end{aligned} \tag{2.5}$$

where b is a parameter (that is assumed to be costant during motion but that can be changed to obtain different types of motion) that measures the friction. Such a term is called *damping* and, in general, it can be also a nonlinear function of v or depend on x. Unlike the conservative case described above, now the pendulum will rotate a certain number of times (depending on initial conditions) and then will swing back and forth with decreasing amplitude, approaching ever closer to the stable equilibrium point $(x, v) = (0, 0)$. The point at the origin is an attractor since all initial conditions in the phase state are drawn to it and it is called a *sink*.

There are clearly other types of attractors. Let us consider for example the case of the Van der Pol oscillator. This system is described by the equation[1]:

$$\ddot{x} + b(x^2 - 1)\dot{x} + x = 0 \tag{2.6}$$

which, in analogy with what has been done so far, can be written as:

$$\begin{aligned} \frac{\mathrm{d}x}{\mathrm{d}t} &= v \\ \frac{\mathrm{d}v}{\mathrm{d}t} &= -b(x^2 - 1) - x \end{aligned} \tag{2.7}$$

In this situation the damping is negative near the origin but becomes positive when we get too far from it. The antidamping that occours implies an external source of energy corresponds to positive feedback. In this case we have a *limit cycle*, where the two effects offset. The initial conditions outside the limit cycle yields a trajectory which converges to this attractor and circulates in periodic motion in the limit $t \to +\infty$. In the same way, the initial conditions inside the limit cycle spirals outwards, asymptotically approaching the latter. Actually, the point at the origin taken as initial condition, does not generate a trajectory that asymptote to the limit cycle because it is still an equilibrium point (now unstable, and called *repellor*). However, for physical real systems this fact is not important because the presence of noise and fluctuations (that move the system from equilibrium) is unavoidable.

The two types of attractors discussed are qualitatively represented in Fig. 2.1.

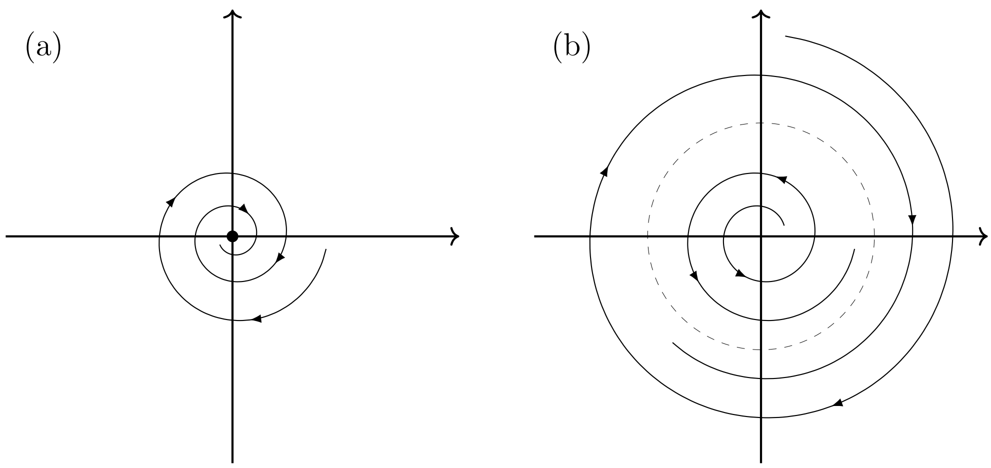

Figure 2.1: (a) The point at the origin is an attractor (sink). (b) The dashed circle is the attractor (limit cycle).

[1]This equation, obtained by the physicist Balthasar Van der Pol in the 1920s, has been use to model heartbeats, pulsating stars, neuronal activity, earthquakes, bipolar disorders and many other phenomena.

2.4 Chaos

Working with deterministic dynamical systems we can have *linear* systems, for which the superposition principle holds[2], and *nonlinear* systems for which this is no longer true. Nonlinearity, for suitable values of the system's parameters, can lead to chaos.

An universally accepted mathematical definition of chaos does not exists but a commonly used definition is the following, originally formulated by Robert L. Devaney [9].

Definition 2.4.1. Let V be a set. $f : V \to V$ is said to be chaotic on V if

(i) f has sensitive dependence on initial conditions.
(ii) f is topologically transitive.
(iii) periodic points are dense in V.

Going into detail:

(i) Sensitivity to initial conditions is a property that characterize chaotic systems and makes their evolution hard to predict. Let us consider two orbits $\mathbf{x}_1(t)$ and $\mathbf{x}_2(t)$ obtained as the time evolution by a continuous dynamical system starting from arbitrarily close initial conditions $\mathbf{x}_1(0)$ and $\mathbf{x}_2(0) = \mathbf{x}_1(0) + \boldsymbol{\delta}(0)$. The system having sensitive dependence on initial conditions means that, in the limit $\|\boldsymbol{\delta}(0)\| \to 0$ and large t, orbits remain bounded and the difference between them $\|\boldsymbol{\delta}(t)\| = \|\mathbf{x}_2(t) - \mathbf{x}_1(t)\|$ increases exponentially, i.e.

$$\frac{\|\boldsymbol{\delta}(t)\|}{\|\boldsymbol{\delta}(0)\|} \approx e^{\lambda t}, \;\; \lambda > 0 \tag{2.8}$$

where λ is called *maximum Lyapunov exponent* (MLE). We note that the request of bounded orbits (that is, exists some ball in phase space which solutions never leave) is particularly important because otherwise, if orbits go to infinity, it would be simple for their distance to diverge exponentially.

The most important consequence of this property is that, as far as we are able to precisely measure the initial state of a system, there will always be a small error (given for example by measuring instruments) which can grow rapidly over time. Therefore, even if we know exactly the deterministic laws governing time evolution, our predictions on the behaviour of the system after a certain time are no longer reliable. Furthermore, if the precision with which we measure the state of the system in the initial instant is improved by a factor of 10, we only gain a $log(10)$ factor for the maximum time for which the predictions are accurate.

Even errors in computation, introduced by round-off, may become magnified and can totally change the solution. It is therefore natural to ask

[2]The equations (2.1) are said to be linear if taken two solutions then any linear combination of them is still a solution.

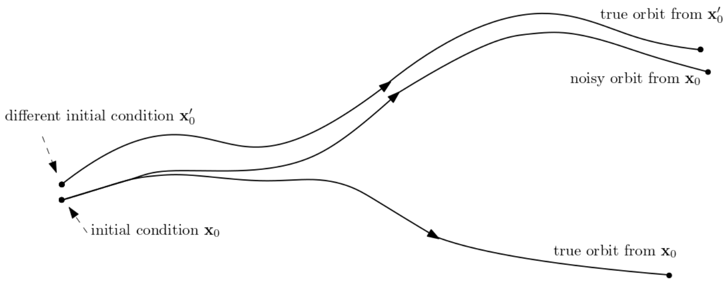

Figure 2.2: Chaotic systems exhibit sensitivity to initial conditions. Two orbits starting from slightly different initial conditions $\mathbf{x}_0$ and $\mathbf{x}_0'$ diverge; the same happens for the true trajectory and the noisy one starting from the same initial condition. Furthermore, the true orbit from $\mathbf{x}_0'$ shadows the noisy orbit from $\mathbf{x}_0$.

whether the simulations performed on computers represent the true behaviour of a dynamical system, and are not instead only the result of chaos-amplified computer round-off. A partial answer to this question is given by the *shadowing* property for certain chaotic systems [10]: as we said, a numerical orbit diverges exponentially from the true one with the same initial condition but there exists a true trajectory with a slightly different initial conditions that stays near (shadows) the numerical trajectory.

(ii) Formally, $f : V \to V$ is said to be topologically transitive if for any pair of open sets $U, W \subset V$ there exists $k > 0$ such that $f^k(U) \cap W \neq \emptyset$, where $f^k(U) = \underbrace{f \circ \ldots \circ f}_{k\text{-times}}(U)$. Intuitively, if a map is topologically transitive then given a point x and a region W, there exists a point y near x whose orbit passes through W. Consequently, the state space of a chaotic system cannot be decomposed into disjoint open sets. We have a sort of ergodicity in the sense that a trajectory eventually connects any region of the space with any other.

(iii) The point $\mathbf{x}$ is a periodic point of period n if $f^n(\mathbf{x}) = \mathbf{x}$. The set of all iterates of a periodic point form a periodic orbit. The density of periodic points in V implies that for any given point in V there is a periodic orbit that passes arbitrarily close to it.

It is clear that, unlike (i), properties (ii) and (iii) are difficult to identify experimentally. However, they have observable consequences. In particular, the time evolution of a chaotic system in state space converges to an object called *strange attractor*, characterized by a *fractal* structure [10]. This means that strange attractors exhibits *self-similarity* and has a non-integer dimensionality.

To understand what it means to have non-integer dimensionality, suppose to consider a fractal object with dimension $1 < D < 2$, for example $D = 1.3$. We know in general that if we have an object of dimension D (assuming that it has a mass density), taking an arbitrary point in it and considering an open ball centered in that point, we can measure the mass contained in the ball as

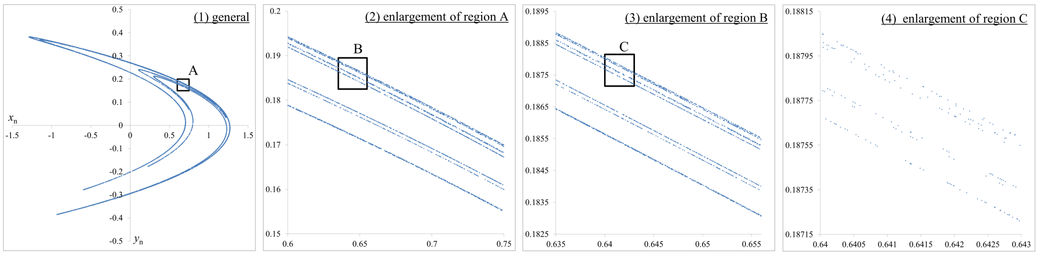

Figure 2.3: The famous Henon attractor exhibit self-similarity: at all magnification levels the same qualitative structures are visible. Source: https://commons.wikimedia.org/wiki/File:Fractal_of_henon_attractor.png

a function of the radius. For small distances $m(r) \propto r^D$. For the same density and radius, the fractal "weights" more than a line but less then a surface, as if a dense set (which is the set of the periodic points) had been removed from the surface.

Self-similarity[3] is the exhibition of similar patterns at increasingly smaller scales and for this reason a fractal does not appear simplified when we see it zoomed. As shown in Fig. 2.3, with each magnification we can see new filaments that were not observable in the previous scale. In principle we can perform this magnification process endlessly but, in practice, the filaments that we are able to see are limited by the precision of the computer used and by computing time.

Sometimes strange attractors are also called chaotic attractors but the two terms are different: *chaos* describes the dynamical property of the attractor (i.e., sensitivity to initial conditions) while *strange* refers to the geometrical properties. There are examples of strange attractors that are not chaotic [12] or viceversa, but they are rare.

To summarize, the sensitive dependence on initial conditions and the presence of strange attractors are fingerprints of chaos and we look for them to identify chaos in an experimental system. Actually, another important property allow us to identify chaos: the trajectory winds around forever never repeating on a strange attractor and the time series arising by chaotic systems are aperiodic and characterized by broad, noise-like Fourier spectra [13].

When we consider a system like (2.1), chaos requires at least three dimensions[4] to occur [10], namely $N \geq 3$, so that the streamlines in the state space can cross by passing behind one another. Indeed, chaos is a dynamical regime deterministic and aperiodic where intersections within the trajectories are not allowed (because of determinism) and the time evolution can't return twice on the same point in the state space (because of aperiodicity).

When we are dealing with maps like (2.2) it is important to distinguish be-

[3]In general, it is more correct to speak of self-affinity because in case of self-similarity, the objects is scaled by the same amount in all space directions, but in self-affinity scaling is not necessary identical in all directions [11].

[4]We can have three first-order differential equations or a third-order differential equation.

tween invertible or noninvertible maps: in the first case there can be chaos if $N \geq 2$ while in the second case chaos is possible even in one-dimensional maps (e.g. the logistic map, that will be presented later) [10].

We already know that a strange attractor is a fractal and, for a three-dimensional chaotic flow, must have a dimension $D < 3$ and $D > 2$ (otherwise it cannot be aperiodic) so it is useful to introduce a method to represent it in a two-dimensional plot. We use a technique called the *Poincarè section* method. The idea is to choose a $(N-1)$-dimensional surface in the state space and observe the intersections of the orbit (and therefore of the strange attractor) with it. For example we can choose as a surface the plane defined by a setting one component of the state $\mathbf{x} = (x^1, x^2, .., x^N)$ to a fixed value. Is it clear that, with this procedure, we reduce the dimension of the attractor by 1.0. The dimension of the Poincarè section is independent of the chosen surface [10].

The method allows to reduce a continuous time system to a discrete map called the *Poincarè map*. For example, we can consider the surface given by the plane $\pi : x^3 = c$ where c is a constant value as represented in Fig. 2.4. The intersections of the flow with this surface are represented with points A, B and C. Point A determines uniquely point B using (2.1) and viceversa (by reversing time). We have got an invertible two-dimensional map.

We note that the minimum dimensional requirements for chaos to occur for continuous or discrete systems are in agreement with these results.

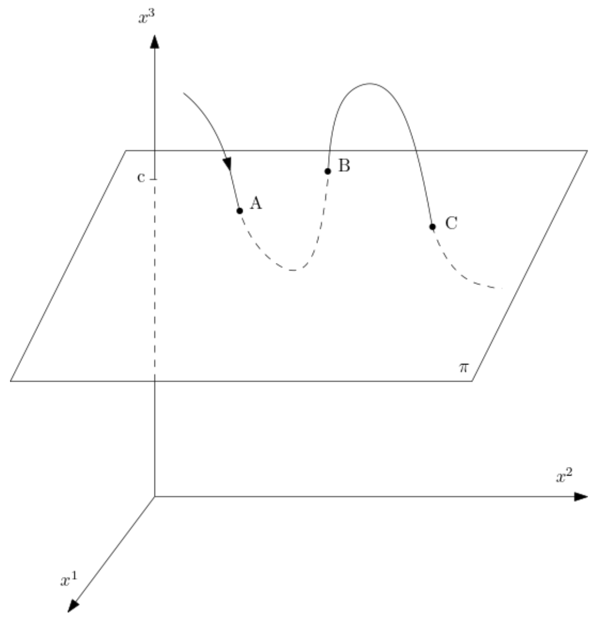

Figure 2.4: Graphical representation of an example of Poincarè section and Poincarè Map.

2.5 Spectrum of Lyapunov Exponents

The sensitivity to initial condition is the main feature of chaos and then it is useful to introduce quantities that allow us to measure (in a quantitative way) this dependence on the initial conditions. As we already mentioned, for a chaotic system two trajectories in the state space which initially are separated by a vector $\boldsymbol{\delta}(0)$ diverge exponentially:

$$\|\boldsymbol{\delta}(t)\| \approx e^{\lambda t}\|\boldsymbol{\delta}(0)\|, \ \lambda > 0 \tag{2.9}$$

where λ is the maximum Lyapunov exponent (MLE).

Different orientations of initial separation vector can produce a different rate of separation thus there isn't only one Lyapunov exponent but a number equal to the dimensionality of the state space: there is a *spectrum of Lyapunov exponents*. To understand what is the role of these Lyapunov exponents, let us suppose to take a spherical ball in a three-dimensional state space. Considering the points contained in this ball as initial conditions, evolving in time it distorts into an ellipsoid. We will have three orthogonal axes of this ellipsoid corresponding to the three independent directions on which one can decompose the generic initial separation vector. Each of these axis expands (or contracts) at a rate given by the correspondent Lyapunov exponent. Thus, the longest axis expands (or less likely contracts) at a rate given by the largest Lyapunov exponent $\lambda = \lambda_1$. Then, if we consider the intersection between the ellipsoid and the plane perpendicular to this axis (which contains the center of the ellipsoid) we obtain an ellipse whose major axis is expanding or contracting at a rate given by the second Lyapunov exponent λ_2 and the minor one at a rate given by λ_3. From this definition, it is clear that $\lambda_1 \geq \lambda_2 \geq \lambda_3$, and this convention is universal [8]. The most important consequence is that knowing the MLE is enough to identify chaos because if it is zero or negative, none of the others can be positive but if it is positive, the system exhibits sensitive dependence on initial conditions (independent of the values of the others). To summarize:

- if $\lambda > 0$ we have sensitive dependence on initial conditions and the system is chaotic.
- if $\lambda = 0$ we have periodicity or *quasiperiodicity*[5].
- if $\lambda < 0$ we have a stable equilibirum.

Finally, let us observe that the reciprocal of the largest exponent, $1/\lambda$, is the *Lyapunov time*, which is the characteristic time scale on which a dynamical system is chaotic and represents the characteristic time when divergences between trajectories become considerable.

In a chaotic system there must be *stretching* that is the exponential separation of trajectories with nearby initial conditions. However, there must be also *folding* to prevent trajectories from going to infinity. Indeed, attractors are bounded sets and this implies also that chaotic systems must also be *recurrent* which means that a trajectory will eventually return arbitrarily close to its starting point (but not exactly otherwise there would be periodicity) and will do it several times. To have folding it can be proved that the presence of at least one nonlinear element

[5]Quasiperiodic motion is the motion of a dynamical system containing a finite number of incommensurable frequencies.

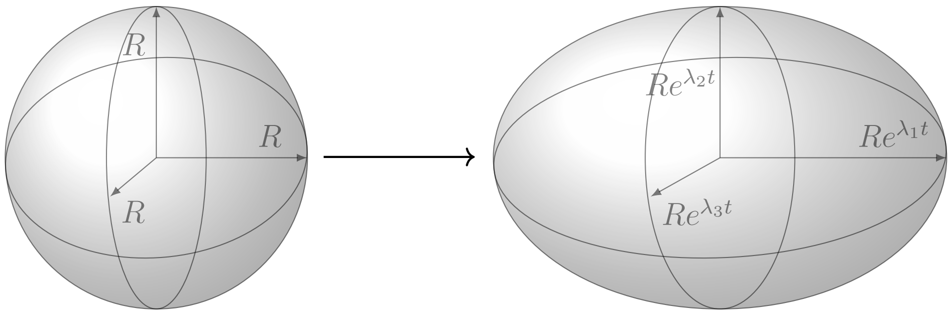

Figure 2.5: A spherical ball of initial conditions becomes an ellipsoid as time increases and the axis of this ellipsoid expand or contract at a rate given by one of the Lyapunov exponents. Note also that continuing stretching in one direction while contracting in another, the ellipsoid become a thin filament that eventually gives rise to a strange attractor.

is necessary [8] and consequently we can have chaos only for nonlinear dynamical systems. However, nonlinearity does not guarantee chaos to occur.

Another property of bounded systems is that, unless the trajectory attracts to an equilibrium point where it stalls and remains forever, the points must continue moving forever with the flow. However, if we consider two initial conditions separated by a small distance along the direction of the flow, they will maintain their average separation forever since they are subject to the exact same flow but only delayed slightly in time. This fact implies that one of the Lyapunov exponents for a bounded continuous flow must be zero unless the flow attracts to a stable equilibrium.

It is important to underline that the volume of the ellipsoid is proportional to the product of its axes and we can write $V = V_0 e^{(\lambda_1+\lambda_2+\lambda_3)t}$. Considering bounded system then the sum of the Lyapunov exponents cannot be positive. The spectrum of Lyapunov exponents can then give much more information about the dynamics of a given system than the only MLE: we can make considerations about the type of attractor and its dimensionality. For example, a *hyperchaotic attractor* is defined as chaotic behaviour with at least two positive Lyapunov exponents. Combined with one null exponent along the flow and one negative exponent to ensure the boundness of the solution, the minimal dimension for a (continuous) hyperchaotic system is 4.

2.6 Bifurcation diagrams

When we speak of chaotic systems, we are typically dealing with dynamical systems dependent on one or more parameters that, for appropriate values of them, exhibit chaotic behaviour. It is therefore interesting to study the mechanisms underlying the transitions of a system towards the chaotic regime and the parameter values for which these occur.

The problem of how a system passes from being nonchaotic to being chaotic as some parameter of the system itself is varied continuously is not easy and it

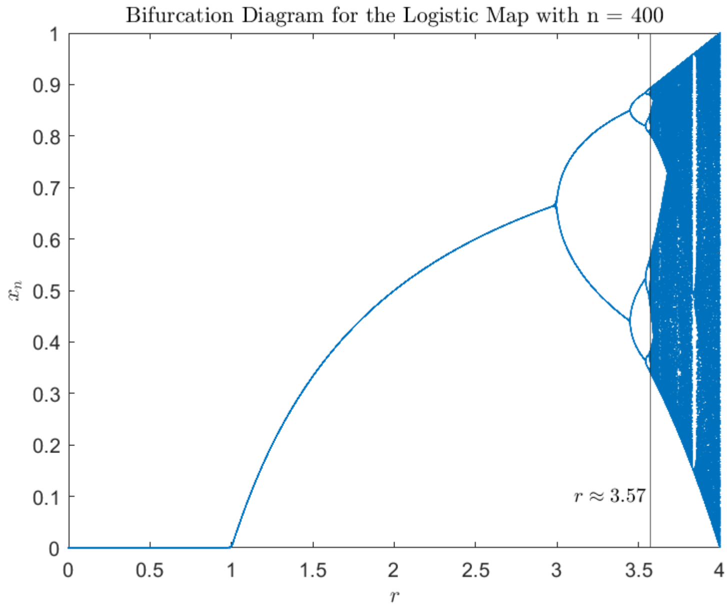

Figure 2.6: Bifurcation diagram of the logistic map.

will not be considered in detail in this thesis work. However, some of the routes by which a system become chaotic are known and in particular there are four important routes to chaos that have been identified and confirmed by numerical and physical experiments [14]. They are *period-doubling cascade*, *intermittency*, *crisis*, and *quasiperiodic routes*. We will not discuss them here, nevertheless it is still useful and interesting to qualitatively study the evolution of the behaviour of a dynamical system as the parameters on which it depends change.

Bifurcation diagrams are a very useful and powerful tool for observing the evolution of a dynamical system. The word *bifurcation* is referred to a sudden qualitative change in the nature of a solution of the system considered, as a parameter is varied [15]. For example we can have a bifurcation at a transition from periodic to quasi-periodic or chaotic regime. The parameter value at which a bifurcation occurs is called a *bifurcation parameter value*. Studying the dynamics of nonlinear systems, bifurcation diagrams are then particularly important because they show the possible long-term values (equilibria/fixed points or periodic/chaotic orbits) of the system as a function of one or more chosen parameters. The concept of bifurcation diagram includes indeed a number of ways of plotting a phase variable on one axis and a parameter on another. An interesting example is the bifurcation diagram (shown in Fig. 2.6) of the *logistic map*[6]:

$$x_{n+1} = rx_n(1 - x_n) \tag{2.10}$$

[6]The map was originally introduced to study the dynamics of populations but was popularized in a 1976 paper by the biologist Robert May called “Simple mathematical models with very complicated dynamics” [16] where the author was interested in showing the surprising range of dynamic behaviour that could be produced by simple and deterministic equations.

On the x-axis are represented the values of the parameter r while on the y-axis are represented the values of x_n obtained for a sufficiently high n (so as to eliminate the initial transient) i.e. the set of values of the map visited asymptotically from initial conditions in the interval $[0, 1]$. It can be seen that for $r \in [0, 1]$ all possible evolutions end with $x_n = 0$. This value therefore represents a stable equilibrium point for the system in this range of values of r. For $r \in (1, 3]$, the system tends to stabilise around a value greater than zero, increasing monotonically with r. If we go over 3, we have an oscillation of x_n initially between 2 values, then between 4, 8, 16, ... until the number of points in the cycle tends to infinity and this happens for $r \approx 3.57$. From this value on, the dynamics becomes chaotic. This transition to chaos through trajectories whose periods double at each bifurcation is the so-called *period-doubling cascade*.

Chapter 3

Chaos in the Burridge-Knopoff Model

We all know what an earthquake is and, probably, we have all felt one at least once in our life. Although it is simple to define an earthquake[1] and the basic mechanism of shallow earthquakes are understood (thanks to the development of plate tectonics), these phenomena are characterized by a rich and interesting dynamics far from being fully understood. One of the central problems in the studies on the dynamics of earthquake faults is the predictability: in this chapter we will present a simple physical earthquake model which is interesting because exhibits a chaotic behaviour [1] and the source of this behaviour is the presence of a nonlinear friction force [18].

3.1 Earthquakes

For our purposes, the Earth can be described as a solid sphere divided in many layers. It has an outer silicate crust which is cold and elastic and called *lithosphere* and under it there is a highly viscous layer called *asthenosphere*. Then it has a solid *mantle*, a liquid *outer core* (whose flow generates the Earth's magnetic field), and a solid *inner core*.

Due to the heat flow from the core, there exists a convection flow in the mantle and the asthenosphere, which is highly turbulent. However, its time scale is of the order of 10^8 years and the spatial extent is of the order of thousand kilometers, so that, within the scales of an earthquake, its motion can be regarded as uniform and constant [19]. Due to the viscosity the convection flow drives different parts of the crust (the tectonic plates) in different directions: this can yield to *stick-slip motion* along the boundary of the plates and then an earthquake. In this framework the stick-slip motion is described using classical mechanics (without considering common phonon modes) as the phenomenon of a sudden jump in the velocity of the movement due to the transition from static friction to kinetic

[1] For example as the shaking of the surface of the Earth resulting from a sudden release of energy in the Earth's lithosphere that creates seismic waves [17].

friction (characterized by a lower friction coefficient).

We can distinguish between two types of earthquakes fault: *transform fault*, where the plates move parallel to the fault and *subduction fault*, where the plates move toward the fault and one of the plates goes under the other [19].

From a physical point of view earthquakes are interesting phenomena because they have a very rich dynamics. An important aspect is that there are many power laws in earthquakes. The most famous one is the Gutenberg-Richter law [20] which states that the earthquake magnitudes are distributed exponentially as:

$$\log_{10}(N) = a - bM \tag{3.1}$$

where M is the magnitude (i.e. the logarithm of the energy released by an earthquake), N is the number of earthquakes having magnitude greater or equal to M, b is a scaling parameter and a is a constant. Another important aspect of earthquakes is their unpredictability: it is impossible[2] to predict these phenomena in any reliable ways. Indeed, the Earth is extremely complex, like the atmosphere, and we know so little about it. Furthermore, it is possible that even if we knew everything about the crust, the mantle etc..., earthquakes would still be unpredictable due to the presence of chaos. We will discuss precisely this point, considering a simple model to investigate nonlinear effects arising in the dynamics of earthquake faults: the *Burridge-Knopoff* model.

3.2 Burridge-Knopoff Model

As mentioned in the previous section, phenomena related to the Earth's crust are very complex and then it is necessary to find a model which is as simple as possible but that exhibits the most important features of the earthquake dynamics. One of the first attempts, studied in many variations, was the model introduced by Burridge and Knopoff in 1967 [21] which we will discuss here.

It consists of a model for a transform fault. In particular, let us consider a one dimensional strip of elastic crust along a fault. This strip can be discretized into a chain of N blocks of equal mass m located along the x axis, as illustrated schematically in Fig. 3.1. We denote by X_j the position of block j with respect to its equilibrium position. Each of these blocks is connected by coil harmonic springs of strength k_c to its two nearest neighbors and we call a the equilibrium spacing between them (when there are no additional forces acting on the system). The blocks are also attached by leaf springs of strength k_p to a surface which moves at constant velocity[3] v. This mechanism corresponds to the slow movement and deformation (far away from the point of contact) of the two tectonic plates whose elastic properties are described by the constants k_p and k_c. The blocks are located on a rough surface (due to the viscosity of the asthenosphere) and they are subject to a frictional force F. The model is a stick-slip

[2] https://www.usgs.gov/faqs/can-you-predict-earthquakes

[3] We consider constant velocity because of the considerations already made on the time scale of the convection flow, which makes the plates move.

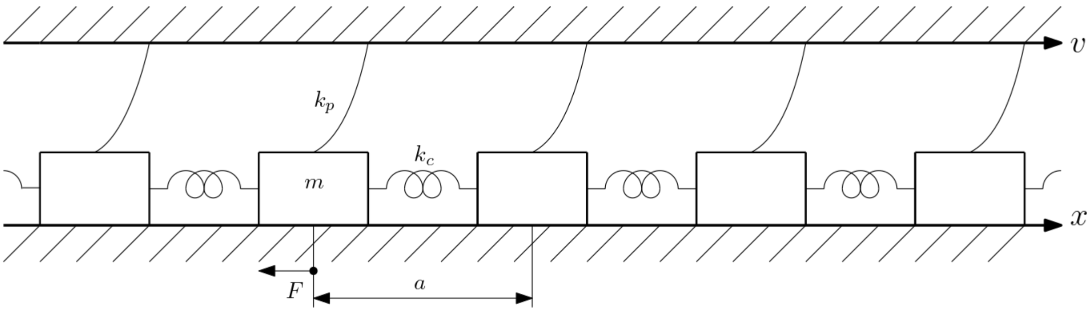

Figure 3.1: Burridge-Knopoff model for the interaction of two crust faults. It consists of a chain of blocks connected by springs. The whole system is pulled with constant velocity on a surface with friction.

model where the blocks are stuck until the pulling forces from the springs overwhelm the static friction and then one or more blocks slide. After sliding (which represent a sort of seismic event) the blocks can stick again in new equilibrium positions until the next slip event. When the spring forces acting on a block are larger than a threshold value F_0, the block can move and it is slowed down by a dynamical friction force which is a function of its velocity. The dynamical friction is weaker than F_0 and thus there exists dynamical instability [18]. The fundamental element of nonlinearity, which is the source of the chaotic behavior of the system, is contained in this velocity weakening friction force $F\left(\frac{\mathrm{d}X_j}{\mathrm{d}t}\right)$ which is assumed to have the form:

$$F\left(\frac{\mathrm{d}X_j}{\mathrm{d}t}\right) = F_0\ \Phi\left(\frac{\mathrm{d}X_j}{\mathrm{d}t}\right) = F_0 \frac{\operatorname{sign}\left(\frac{\mathrm{d}X_j}{\mathrm{d}t}\right)}{1+\left|\frac{\mathrm{d}X_j}{\mathrm{d}t}\right|} \tag{3.2}$$

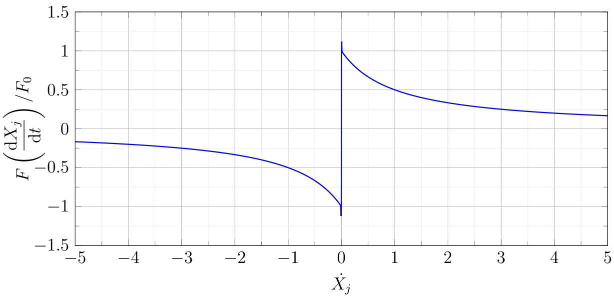

The equation of motion for the j-th block during a slip event are:

$$m\frac{\mathrm{d}^2X_j}{\mathrm{d}t^2} = k_c(X_{j+1}-X_j) + k_c(X_{j-1}-X_j) + k_p(vt-X_j) - F\left(\frac{\mathrm{d}X_j}{\mathrm{d}t}\right) \tag{3.3}$$

$$m\frac{\mathrm{d}^2X_j}{\mathrm{d}t^2} = k_c(X_{j+1}-2X_j+X_{j-1}) + k_p(vt-X_j) - F\left(\frac{\mathrm{d}X_j}{\mathrm{d}t}\right) \tag{3.4}$$

while when the block sticks, one simply has:

$$\begin{cases} \dfrac{\mathrm{d}^2 X_j}{\mathrm{d}t^2} = 0 \\ \dfrac{\mathrm{d}X_j}{\mathrm{d}t} = v \end{cases} \tag{3.5}$$

It has been shown both experimentally [21] and numerically [18] that this model gives rise to events of all sizes and the distribution of earthquakes results in a power-law spectrum similar to what observed in nature (Gutenberg-Richter law).

Earthquakes features have been studied also using the cellular automata (CA) technique but the model considered in this work has an advantage compared to it [18]. The cellular automata is indeed deterministic, such as the Burridge-Knopoff (BK) model (initial conditions are instead random for both models). However, the CA is essentially a kind of simplification of the BK model, made to deal with a very large number of units, which would be impractical by solving differential equations. Therefore, we cannot see and investigate the "true" dynamics because the CA technique admits only two states, stick and slip, and it is then impossible, strickly speaking, to look for chaos. Thus, we will study a symmetric two-block Burridge-Knopoff model and, in particular, we will show that the configuration is chaotic, in agreement with the results of de Sousa Vieira [1]. This outcome is interesting because there exist studies, like the one carried out by Lacorata and Paladin [22], that found chaotic behaviour only with the presence of an asymmetry in the system. However, experimentally has been showed by Field *et al.* [23] (by modeling the BK system with electronic circuits) that a completely symmetric two-block model does actually exhibit chaotic behaviour in a wide range of parameter values. Before going on, we note that a one-block BK model cannot present chaos because it has dimensionality smaller than three.

3.3 Symmetric Two-block Burridge-Knopoff Model

Let us consider the symmetric two-block BK model represented in Fig. 3.2.

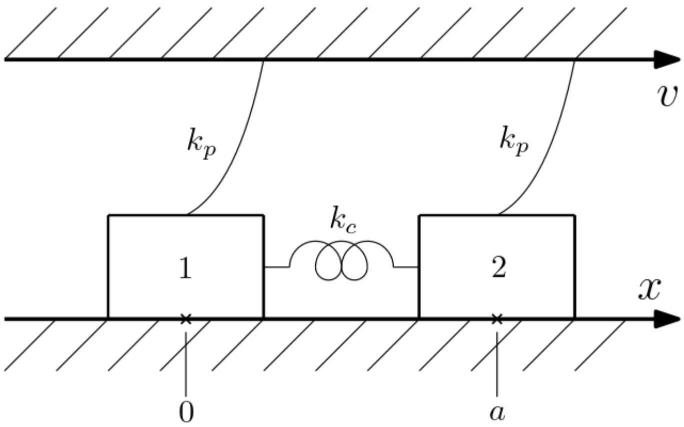

Figure 3.2: Symmetric two-block Burridge-Knopoff model. The system ehibits chaotic behaviour in a wide region of the parameter space.

We now work in the inertial rest frame of the rough surface: we have fixed an origin of the x-axis (parallel to the pulling velocity v) and X_j denotes now the position of block j with respect to this origin. For the sake of simplicity, this zero has been set at the equilibrium position of the first block. The equations of motion of the system are then the following:

$$\begin{cases} m\dfrac{\mathrm{d}^2X_1}{\mathrm{d}t^2} = k_c(X_2 - X_1 - a) + k_p(vt - X_1) - F_0\ \Phi\left(\dfrac{\mathrm{d}X_1}{\mathrm{d}t}\right) \\ m\dfrac{\mathrm{d}^2X_2}{\mathrm{d}t^2} = -k_c(X_2 - X_1 - a) + k_p(a + vt - X_2) - F_0\ \Phi\left(\dfrac{\mathrm{d}X_2}{\mathrm{d}t}\right) \end{cases} \tag{3.6}$$

In order to perform numerical simulations of the system it is useful to rewrite these equations in the dimensionless form. Let us focus only on the first equation of (3.6) since for the second we proceed in an analogous way. We can introduce the adimensional time variable $\tau \doteq \omega_p t$ where $\omega_p^2 \doteq k_p t/m$. Thus, we have:

$$m\omega_p^2\frac{\mathrm{d}^2X_1}{\mathrm{d}\tau^2} = k_c(X_2 - X_1 - a) + k_p(vt - X_1) - F_0\ \Phi\left(\omega_p\frac{\mathrm{d}X_1}{\mathrm{d}\tau}\right) \tag{3.7}$$

$$\frac{k_p}{F_0}\frac{\mathrm{d}^2X_1}{\mathrm{d}\tau^2} = \frac{k_c}{F_0}(X_2 - X_1 - a) + \frac{k_p}{F_0}(vt - X_1) - \Phi\left(\omega_p\frac{\mathrm{d}X_1}{\mathrm{d}\tau}\right) \tag{3.8}$$

Furthermore, we can also rewrite the friction force in terms of $\Phi\left(\omega_p\dfrac{\mathrm{d}X_1}{\mathrm{d}\tau}\dfrac{1}{v_c}\right)$ where v_c is a characteristic velocity. Then, introducing the variables $U_j \doteq k_pX_j/F_0$, $k \doteq k_c/k_p$ and $\alpha \doteq k_pa/F_0$ and denoting differentiation with respect to τ with dots, we obtain:

$$\ddot{U}_1 = k(U_2 - U_1 - \alpha) + \left(v\frac{k_p}{F_0}\frac{\sqrt{m}}{\sqrt{m}}t - U_1\right) - \Phi\left(\omega_p\frac{\mathrm{d}X_1}{\mathrm{d}\tau}\frac{1}{v_c}\right) \tag{3.9}$$

which can be lastly rewritten in the dimensionless form:

$$\ddot{U}_1 = k(U_2 - U_1 - \alpha) + (\nu\tau - U_1) - \Phi\left(\frac{\dot{U}_1}{\nu_c}\right) \tag{3.10}$$

with $\nu \doteq v/V_0$, $\nu_c \doteq v_c/V_0$ and $V_0 \doteq F_0/\sqrt{k_pm}$. To sum up, the equations of motion for the two-block system (3.6) can be written in the following dimensionless form:

$$\begin{cases} \ddot{U}_1 = k(U_2 - U_1 - \alpha) + (\nu\tau - U_1) - \Phi\left(\dfrac{\dot{U}_1}{\nu_c}\right) \\ \ddot{U}_2 = -k(U_2 - U_1 - \alpha) + (\alpha + \nu\tau - U_2) - \Phi\left(\dfrac{\dot{U}_2}{\nu_c}\right) \end{cases} \tag{3.11}$$

Before continuing, we stress that these equations are valid only during the slip events (so when block j is moving) while, when the j-th block is stuck, we simply have $\ddot{U}_j = 0$ and $\dot{U}_j = \nu$.

For each of the two blocks there exists also an equilibrium point which can be found by taking $\ddot{U}_j = 0$ and $\dot{U}_j = \nu$ in Eq. (3.11). In this way we have:

$$\begin{cases} k(U_2^{eq} - U_1^{eq} - \alpha) + (\nu\tau - U_1^{eq}) - \Phi\left(\dfrac{\nu}{\nu_c}\right) = 0 \\ -k(U_2^{eq} - U_1^{eq} - \alpha) + (\alpha + \nu\tau - U_2^{eq}) - \Phi\left(\dfrac{\nu}{\nu_c}\right) = 0 \end{cases} \tag{3.12}$$

and by adding and subtracting the two equations we obtain the following system:

$$\begin{cases} 2\nu\tau - U_1^{eq} - U_2^{eq} + \alpha - 2\Phi\left(\dfrac{\nu}{\nu_c}\right) = 0 \\ (2k+1)(U_2^{eq} - U_1^{eq} - \alpha) = 0 \end{cases} \tag{3.13}$$

whose solutions, it is easy to prove, are:

$$U_1^{eq} = \nu\tau - \frac{\nu_c}{\nu_c + \nu} \quad \text{and} \quad U_2^{eq} = \nu\tau - \frac{\nu_c}{\nu_c + \nu} + \alpha \tag{3.14}$$

The stability of such a solution, for any number of blocks, was analyzed in detail by Carlson and Langer [18] and U_j^{eq} for $j = 1, 2$ are unstable equilibrium points around which the orbits of block j circle in phase space.

3.4 Numerical Methods and Results

We want now to study the dynamical behaviour of the symmetric two-block BK model discussed so far and to do it we perform numerical simulations of the system.

It is important, in these tests, to distinguish whether the block is moving (and then is subject to the velocity weakening friction force in Eq. (3.2)) or not (and then its acceleration is equal to zero). To do so, we will say that the block 1 is moving if its velocity $\dot{U}_1$ is non-zero or, otherwise, if the absolute value of the sum of the elastic force $F_{el} = k(U_2 - U_1 - \alpha)$ and the driving force $F_{dr} = (\nu\tau - U_1)$ is greater than $\Phi(0) = 1$, which is the static friction force acting on the block. In this last case indeed the block starts sliding. In the same way, we say that the block 2 is moving if $\dot{U}_2 \neq 0$ or if $\dot{U}_2 = 0$ but at the same time $|-k(U_2 - U_1 - \alpha) + (\nu\tau - U_2)| > 1$.

So we work with the four dimensionless variables U_1, $\dot{U}_1$ and U_2, $\dot{U}_2$ and said F_{tot_1} and F_{tot_2} the total dimensionless forces acting on block 1 and 2, in our simulations, we numerically solve the following system of ordinary differential equations:

$$\begin{cases} \dot{U}_1 = V_1 \\ \dot{V}_1 = F_{tot_1} \\ \dot{U}_2 = V_2 \\ \dot{V}_2 = F_{tot_2} \end{cases} \tag{3.15}$$

where $F_{tot_j} = 0$ if block j is not moving, otherwise it is given by the sum of the elastic force, the driving force and the dynamic friction force acting on that block. We also note that the system depends on the parameter k, ν, ν_c and α. Unless explicitly stated otherwise, we take in the numerical tests $k = 1$, $\nu = 0.1$ and $\alpha = 10$. However, similar behaviour to the one which will be discussed was found for other parameter values as well. For example, realistic values of ν are of order of 10^{-8} or less, that is the existing ratio between the typical duration of a seismic event and the average recurrence time, but the main qualitative results are independent of ν [22].

Furthermore in our studies, to reduce numerical errors and to take into account that kinetic friction is smaller than static friction, we will introduce another parameter σ in the expression of the velocity weakening friction force:

$$\Phi(V_j) = \frac{\text{sign}(V_j)}{1 + |V_j|/\nu_c}(1 - \sigma) \tag{3.16}$$

and in particular we will consider $\sigma = 0.1$.

The numerical simulations show a rich dynamics of the system and the presence of both periodic, quasiperiodic and chaotic behaviour in agreement with de Sousa Vieira [1].

We implemented the numerical tests using MATLAB and, to achieve better precision and efficient computation, we used the built-in ODE solver `ode45`, which implements a Runge-Kutta(4,5) method with a variable time step. The initial conditions used here are the blocks initially at rest with block 1 in its equilibrium position and block 2 slightly offset (by a small random displacement) from its equilibrium position. In all the simulations a transient time of 500 in units of τ (chosen by visually inspecting the phase space evolution) was discarded. Furthermore, backward motion of the blocks was allowed and then we can have negative velocities. However, comparing the results obtained here with those of de Sousa Vieira [1] where backward motion is not allowed, we see that they remain essentially the same and the main features of the dynamics are identical.

In Fig. 3.3a we show an example of chaotic orbit, by plotting $\dot{U}_1$ versus $U_1 - U_1^{eq}$, in the case of $1/\nu_c = 1$.

Furthermore, we see from Fig. 3.3b that the plot of $\dot{U}_2$ versus $U_2 - U_2^{eq}$ is identical to the one of Fig. 3.3a, showing that the two blocks considered here will visit the same region of the phase space, but not necessarily at the same time. For this reason, from now on, only block 1 will be considered and we will denote for simplicity $U_1^{eq} \equiv U_{eq}$.

These first results already highlight the fact that the system admits a chaotic dynamic regime. Indeed, as can be seen, the orbits of the two blocks in the phase space give rise to strange attractors which are bounded and where we can easily see recurrence, as the system repeatedly returns to states arbitrarily close to the starting one. We also note that, as expected, the trajectory of block j circles around the unstable equilibrium point U_j^{eq} which is obtained by taking $\dot{U}_j = \nu = 0.1$.

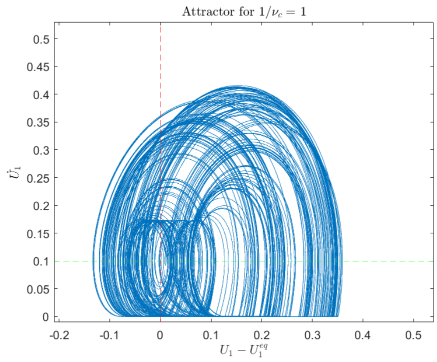

(a) The trajectory in phase space for block 1 when $1/\nu_c = 1$ forms a strange attractor.

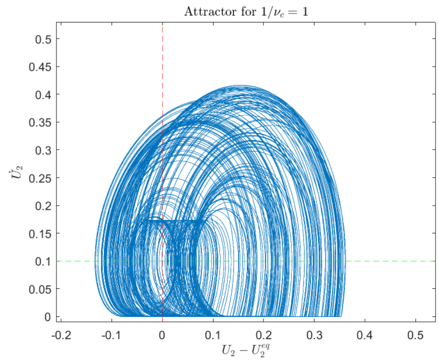

(b) The trajectory in phase space for block 2 is essentially the same as the one of block 1.

Figure 3.3: Chaotic orbits in phase space for the two blocks in the symmetric Burridge-Knopoff model.

3.4.1 Bifurcation Diagrams

As described in Section 2.6, it is interesting to study the nature of the solutions admitted by a dynamical system as a parameter of the system itself varies. In particular, we are interested in understanding for which values of a given parameter the system exhibits chaotic behaviour, and in studying the transitions by which a dynamical system goes from being nonchaotic to becoming chaotic or vice versa. In the particular case of the system under investigation, we want to understand for which values of the dimensionless characteristic velocity, or rather of $1/\nu_c$ which is connected to the natural (adimensional) time unit of the system[4], the solutions become chaotic.

To this end, two bifurcation diagrams for the symmetric two-block system are shown in Fig. 3.4. To obtain these diagrams we first generated the system time series for 100 different values of $1/\nu_c$ equispaced between 0 and 1.5 (in addition to the one already produced by numerically integrating the equations of the system in the case $1/\nu_c = 1$). The initial conditions used here are the same as those described in the previous section and we have used a fixed time step δt in the solver because we then want to perform the FFT (Fast Fourier Transform) for some of these time series. Next, for the first graph, we looked for the two immediately following time instants t_1 and $t_1 + \delta_t$ for which $\dot{U}_1(t_1) > 0.1$ and $\dot{U}_1(t_1) < 0.1$ (so, when the trajectory crosses from top to bottom the horizontal line corresponding to $\dot{U}_1 = 0.1$) and we considered as U_1 the mean value given by $(U_1(t_1) + U_1(t_1 + \delta t))/2$. In a similar way, we also built the second graph, but considering as $\dot{U}_1$ the average of the values that occur when the trajectory crosses from left to right the vertical line corresponding to $U_1 - U_{eq} = 0$.

It can be seen from the diagrams that the nature of the dynamics of the system changes a lot. There are regions (corresponding to certain intervals of the

[4]In our model $1/\nu_c$ is indeed linked to earthquakes' time scale.

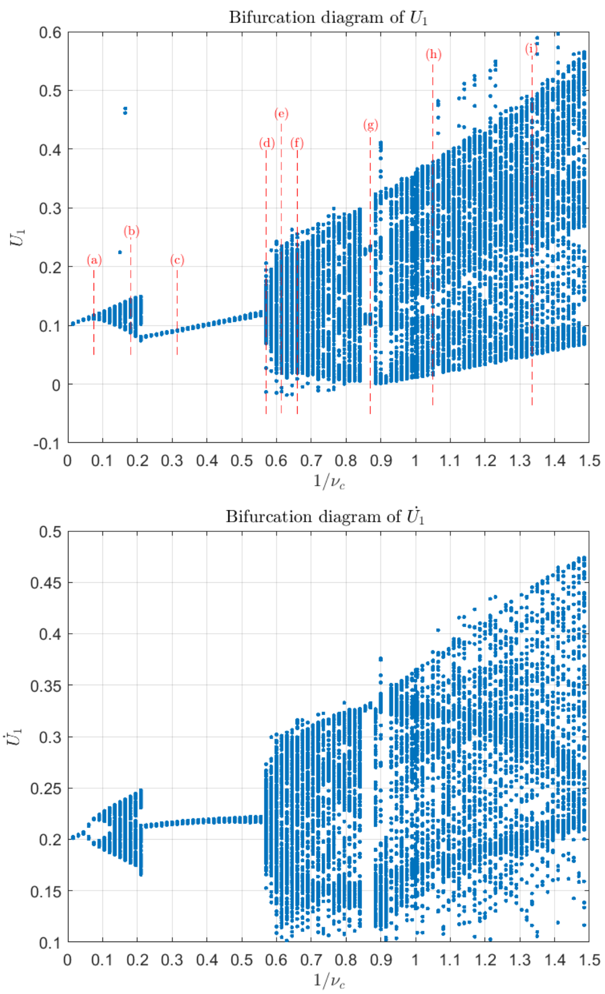

Figure 3.4: Bifurcation diagrams for the symmetric two-block system. The above diagram is the bifurcation diagram of U_1 in the Poincarè section in which $\dot{U}_1 = 0.1$. The one below is the bifurcation diagram of $\dot{U}_1$ in the Poincare section in which $U_1 - U_{eq} = 0$. The red lines shown in the first diagram correspond to the values of the parameter $1/\nu_c$ for which the system's strange attractor will be plotted below (Fig. 3.5) and the corresponding time series FFT (Fast Fourier Transform) will be performed.

parameter $1/\nu_c$) in which the system is characterised by periodic, quasiperiodic and chaotic behaviour [1]. In order to study more in detail the transitions towards chaos we show in Fig. 3.5 the orbit in phase space for block 1 when 9 different values of $1/\nu_c$ (labelled as (a)-(i) in Fig. 3.4) are taken into account. It is easy to understand when we are faced with a strange attractor or a periodic trajectory. For example in case (a) and (c) the system is periodic (in (a) with period-2 cycle) as it would seem to be in (g). The first strange attractor, on the other hand, appears in (b) while for $1/\nu_c > 1$ attractors of gradually increasing size, such as (h) and (i), take shape.

In addition, to distinguish between periodic or chaotic regime, we have also performed the Discrete Fourier Transform (using a FFT algorithm) of the time series of U_1. We used as sampling time $\delta t = 0.01$ and then frequency is expressed in terms of δt^{-1} and the Nyquist frequency is $f_{Nyq} = 1/(2\delta t)$. The results obtained are interesting because we expect to have in the frequency domain a signal characterised by one or more well defined peaks in the case of periodic behaviour while, in the chaotic case, a broad and noise-like signal and then we can qualitatively see the the type of behaviour of the system.

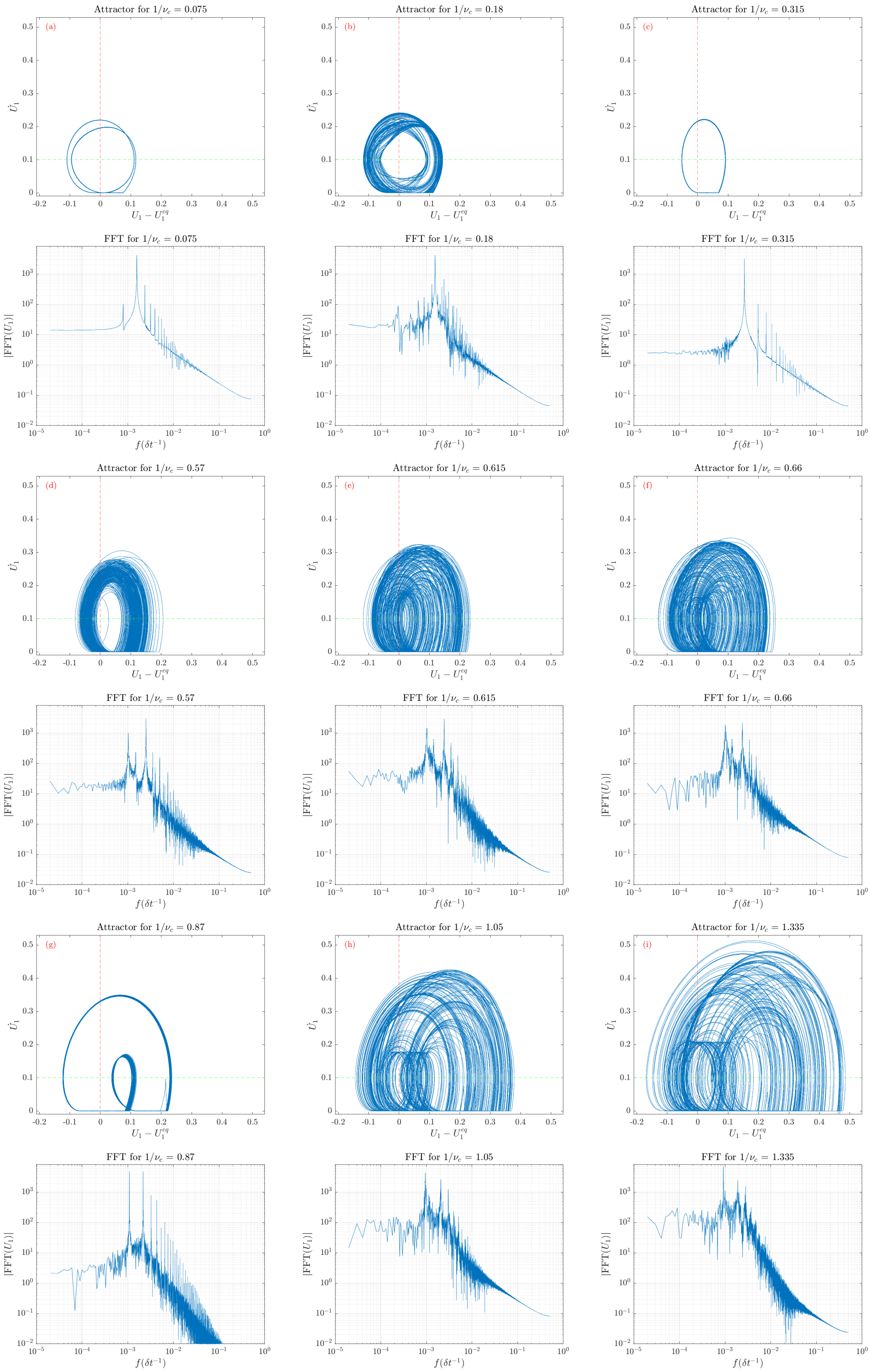

Figure 3.5: Orbits of block 1 and Fast Fourier Transform (FFT) of U_1 time series for different values of $1/\nu_c$. It can be seen how the behaviour of the system changes and evolves for 9 different values of $1/\nu_c$.

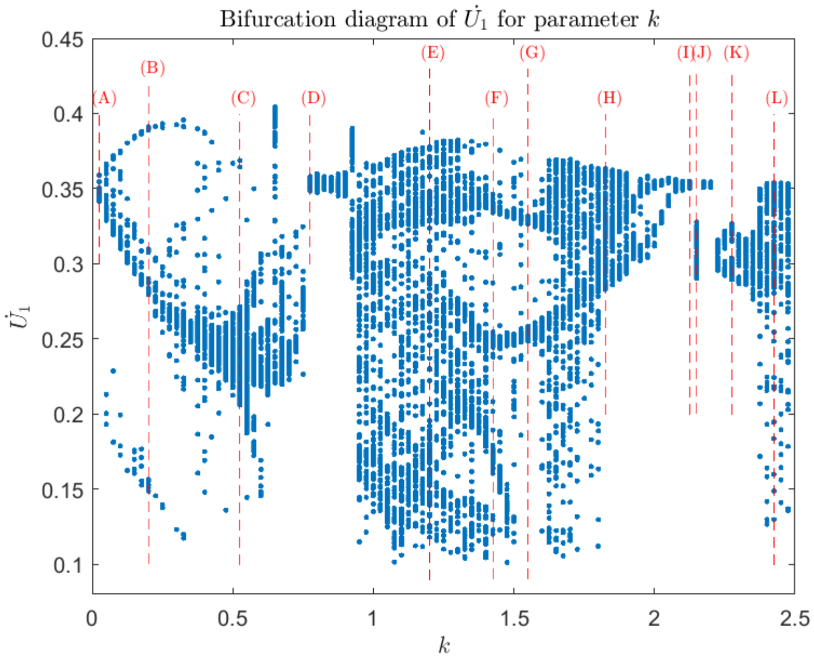

Figure 3.6: Bifurcation diagram for the symmetric two-block system when k varies in $[0, 2.5]$. The dotted red lines shown correspond to the values of k for which the system's strange attractor will be plotted below (Fig. 3.7).

We emphasise that the presence of quasiperiodic regimes has not been quantitatively demonstrated here due to the difficulty of obtaining the sprectrum of Lyapunov exponents (as will be explained in the following section). However, according to de Sousa Vieira [1], quasiperiodic motion occurs after periodic motion, just before the second transition to chaos (which is for $1/\nu_c$ around 0.6), when the maximum and the second largest Lyapunov exponents are both zero. In the same paper, the first entrance to chaos (which occurs at $1/\nu_c \approx 0.112$) was investigated and it would appear that the route to chaos is unusual, from period-1 to period-2 cycle and then directly into chaos. This behaviour can also be qualitatively seen from Fig. 3.4 and Fig. 3.5.

Finally we have also investigated how the behaviour of the system changes as k varies in the range $[0, 2.5]$, while $1/\nu_c$ is now constant and set to 1. Again, we have many different dynamical regimes and in particular there are cases where the system is periodic and cases where it is chaotic, as can be seen from Fig. 3.6. The diagram was obtained in a similar way to the previous ones, considering now the time series for 100 values of k[5] equispaced between 0 and 2.5 (and with $1/\nu_c = 1$).

In order to follow the evolution of the system we have also considered 12

[5]We recall that $k = k_c/k_p$, i.e. it is the ratio between the elastic constant of the harmonic springs (that connect blocks together) and the elastic constant of the leaf springs (that connect blocks to the upper moving surface). The parameter it is then linked, in our model, to the local elastic properties of the two tectonic plates.

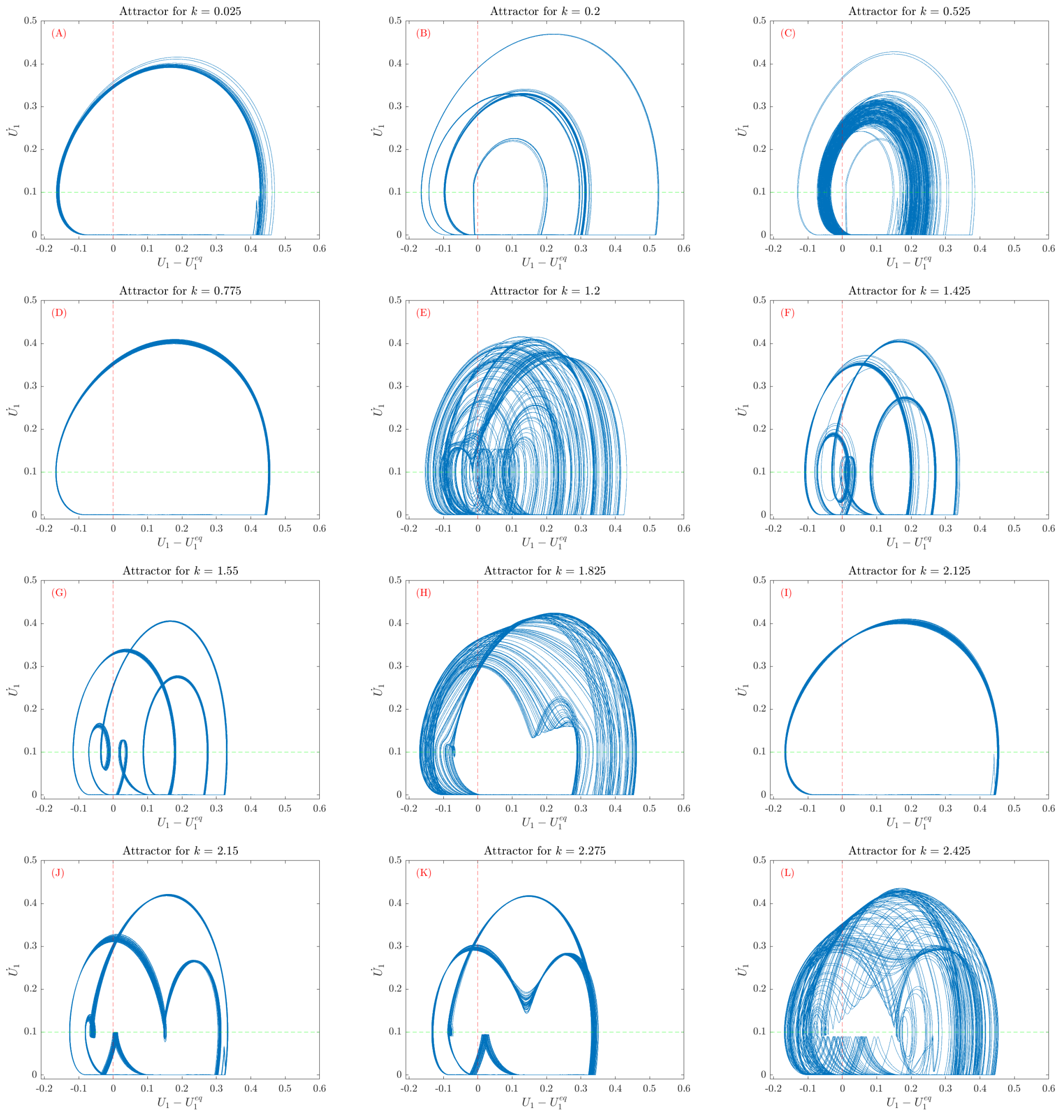

Figure 3.7: Orbits in phase space for block 1 for 12 different values of k and with $1/\nu_c = 1$.

different values of k and, for each of them, plotted the orbit for block 1. The results obtained are shown in Fig. 3.7. One can qualitatively observe that there are several k intervals in which the system is periodic (with not only period-1 cycles) alternating with situations in which instead chaos is evident.

3.4.2 Maximum Lyapunov Exponent

In order to quantitatively characterize the dynamics and demonstrate the presence of chaos, we have calculated the Maximum Lyapunov Exponent (MLE) of the system for $1/\nu_c = 1.05$. The trajectory in phase space for block 1 is shown in Fig. 3.5(h).

The reason why we have considered only the MLE and only one value of the parameter $1/\nu_c$ is that the dynamics of the system is based on the stick-slip phenomenon and the blocks spend most of the time standing still. Consequently, the standard techniques typically used to calculate the spectrum of Lyapunov exponents (such as the Benettin algorithm) do not work effectively. In this work then we performed just an estimate of the MLE.

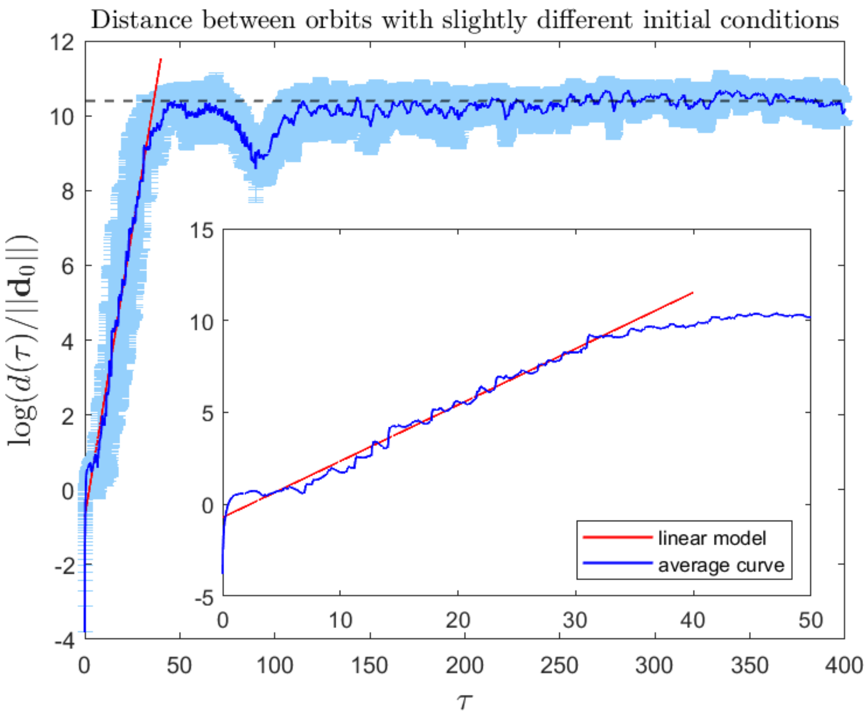

Figure 3.8: Average curve of $\log(d(\tau)/\|\boldsymbol{d}_0\|)$ versus τ plotted with error. It is also shown a magnification of the linear region with the best linear fit. The black dotted line represent the mean value of the plateau.

To do this we have firstly generated two initial conditions $\boldsymbol{U}(0) = (U_1(0), U_2(0), \dot{U}_1(0), \dot{U}_2(0))$ and $\boldsymbol{U}_d(0) = (U_{1d}(0), U_{2d}(0), \dot{U}_{1d}(0), \dot{U}_{2d}(0))$ which differs by $\boldsymbol{d}_0 = (0, \epsilon, 0, 0)$ where $\epsilon = 10^{-5}$, so that $\boldsymbol{U}_d(0) = \boldsymbol{U}(0) + \boldsymbol{d}_0 = (U_1(0), U_2(0) + \epsilon, \dot{U}_1(0), \dot{U}_2(0))$. In principle, $\boldsymbol{d_0}$ could be any initial displacement vector, with norm arbitrarily small. Then, starting from $\boldsymbol{U}_d(0)$ and $\boldsymbol{U}(0)$ we have numerically integrated the equations of the system (3.11) and then taken into account the time evolution $\boldsymbol{U}_d(\tau)$ and $\boldsymbol{U}(\tau)$. For each (discrete) time instant we can then evaluate the distance between the two orbits by computing $d(\tau) = \|\boldsymbol{U}(\tau) - \boldsymbol{U}_d(\tau)\|$ where $\|\cdot\|$ is the Euclidean norm. According to what said in Chapter 2, we can plot $\log\left(\frac{d(\tau)}{\|\boldsymbol{d}_0\|}\right)$ versus t: if the system is chaotic we expect to observe a linearly increasing trend at the beginning and then to reach a plateau, since strange attractors are bounded objects and the distance between two orbits can at most be equal to the diameter of the attractor itself. Once the linear region has been identified we can then estimate the MLE by simply performing a linear regression and taking the angular coefficient. This is the MLE in sampling time units λ.

In the simulations we have used $k = 1$, $1/\nu_c = 1.05$, $\nu = 0.1$, $\alpha = 10$, $\sigma = 0.1$ and a fixed time step $\delta t = 0.01$. Furthermore, in the case under examination, it can be seen that growth occurs rapidly and to define a linear region we have considered the value of the plateau (i.e. the value at which the logarithm stabilises), obtained as a mean[6] of the last points (corresponding to a time interval of 200 in units of τ), and we have taken the region where the logarithm goes from 20% to 80% of this value.

In order to get a better estimate of the MLE λ (and its error $\delta\lambda$), we did repeated tests, using two slightly different methods.

In the first case we have performed what described above $N = 100$ times in order to have N MLE estimates λ_i (with error $\delta\lambda_i$ given by the linear regression) with $i = 1, ..., 100$. To get the final estimate of λ, we took the weighted mean of them with its error and obtained $\lambda = 0.23 \pm 0.04$.

In the second case we have numerically integrated $N = 100$ times the equations of the system in order to generate N different time series of $\log(d(\tau)/\|\boldsymbol{d}_0\|)$. We then built an average curve (taking errors into account) and performed a single linear regression on it. This method is way faster then the previous one and in this case we obtained $\lambda = 0.306 \pm 0.009$ which is compatible with the one of the first method. Figure 3.8 shows the average curve with a magnification of the linear region.

What is important is that the estimates made show that, for the parameters considered, there is a linear growth and the MLE is positive and so the system is chaotic.

3.5 Three-block Burridge-Knopoff Model

Let us consider now the three-block BK system, schematically represented in Fig. 3.9.

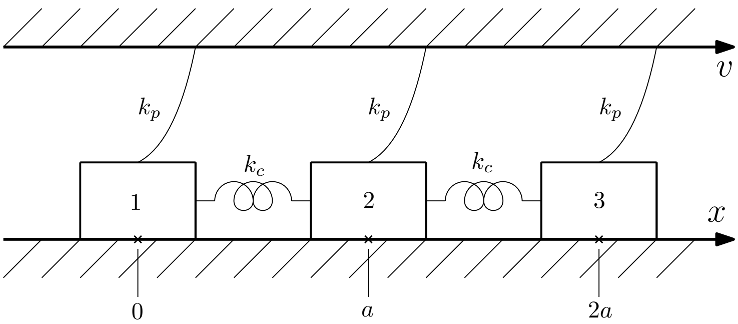

Figure 3.9: Three-block Burridge-Knopoff model.

[6]The trend is not exactly strictly monotonic increasing (the orbits diverge on average) but there are oscillations due to the fact that the system is confined and there are moments when the trajectories come close together again. These oscillations also remain in the plateau and for this reason we have to take a mean value.

The equations of motion are now the following:

$$\begin{cases} m\dfrac{\mathrm{d}^2X_1}{\mathrm{d}t^2} = k_c(X_2 - X_1 - a) + k_p(vt - X_1) - F_0\ \Phi\left(\dfrac{\mathrm{d}X_1}{\mathrm{d}t}\right) \\ m\dfrac{\mathrm{d}^2X_2}{\mathrm{d}t^2} = -\ k_c(X_2 - X_1 - a) + k_c(X_3 - X_2 - a) \\ \qquad\qquad + k_p(a + vt - X_2) - F_0\ \Phi\left(\dfrac{\mathrm{d}X_2}{\mathrm{d}t}\right) \\ m\dfrac{\mathrm{d}^2X_3}{\mathrm{d}t^2} = -\ k_c(X_3 - X_2 - a) + k_p(2a + vt - X_3) - F_0\ \Phi\left(\dfrac{\mathrm{d}X_3}{\mathrm{d}t}\right) \end{cases} \tag{3.17}$$

which can be rewritten in dimensionless form, using the same definitions given in Section 3.3:

$$\begin{cases} \ddot{U}_1 = k(U_2 - U_1 - \alpha) + (\nu\tau - U_1) - \Phi\left(\dfrac{\dot{U}_1}{\nu_c^1}\right) \\ \ddot{U}_2 = k(U_1 - 2U_2 + U_3) + (\alpha + \nu\tau - U_2) - \Phi\left(\dfrac{\dot{U}_2}{\nu_c^2}\right) \\ \ddot{U}_3 = k(U_3 - U_2 - \alpha) + (2\alpha + \nu\tau - U_3) - \Phi\left(\dfrac{\dot{U}_3}{\nu_c^3}\right) \end{cases} \tag{3.18}$$

The difference is that now the system is not necessarily symmetric and, for example, ν_c^1 can be different from ν_c^2 and ν_c^3. Furthermore, we stress that, also in this case, the equations above are valid only during slip events while, when the j-th block is stuck, one simply have $\ddot{U}_j = 0$ and $\dot{U}_j = \nu$. In the numerical simulations we used analogous methods as the case of the two-block model and also in this case chaos has been found in the system. In Fig. 3.10 we show an example of chaotic orbit, by plotting $\dot{U}_1$ versus $U_1 - U_1^{eq}$ (where U_1^{eq} is the same of Section 3.3) in the case of $1/\nu_c^1 = 1/\nu_c^3 = 4/\nu_c^2 = 1.13$ and $k = 1$, $\nu = 0.1$, $\alpha = 10$, $\sigma = 0.1$.

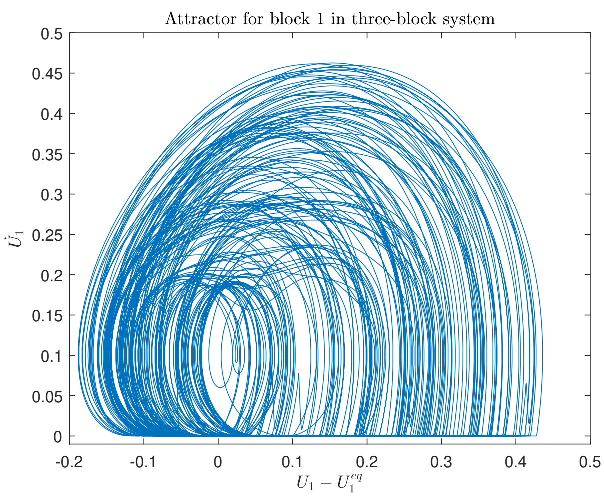

Figure 3.10: The trajectory in phase space for block 1 in the case of $1/\nu_c^1 = 1/\nu_c^3 = 4/\nu_c^2 = 1.13$ forms a strange attractor. The same happens for block 2 and 3.

We will not investigate this system in more detail, but it is interesting to see why it might be useful to do so later. As reported by de Sousa Vieira [1], the phenomenon of *synchronized chaos* appears in the three-block BK model (when there is an asymmetry) in a wide range of the parameter space. Chaotic synchronization refers to a process wherein two (or many) chaotic systems adjust a given property of their motion to a common behavior due to a coupling or to a forcing (periodical or noisy) [24]. The phenomenon cannot occur in the case of two blocks because, if they were synchronised, they would behave as one block and thus the system would be equivalent to the one-block model, which cannot have chaotic behaviour (due to its dimensionality). However, we see from (3.18) that the equations that govern the motion of blocks 1 and 3 have the same functional form and the two blocks are also linked to a common subsystem which is block 2 and then, in this case, there are the ingredients for chaotic synchronization to occur. For this to happen in a large region of the parameters space we have to consider the asymmetric model: if all the parameters' values are the same for each block, it is clear that blocks 1 and 3 are more loose than block 2 and then they attain larger velocities and (with the friction force used) are more unstable but chaotic synchronization are more likely to occur when the subsystems to be synchronized are more stable than the subsystem to which they are connected [25]. For this reason, we have considered the friction force acting on block 2 smaller than the ones acting on blocks 1 and 3 (which means that they are more rough). It is also useful to consider $1/\nu_c^1 = 1/\nu_c^3$ if the goal is to obtain perfect synchronization in the absence of control.

Chapter 4

Conclusions

In the present thesis work, a simple model of an earthquake fault, the so-called Burridge-Knopoff model, was numerically investigated. The work was aimed at the identification of chaos in the symmetric, two-block version of the system. The existence of chaos in earthquake dynamics is an interesting problem because, up to now, accurate predictions of seismic events are impossible and the study of simple models describing the Earth's crust and its phenomenology can be important. Earthquakes are non-periodic phenomena but if their irregular behaviour is caused by a chaotic process (ruled by deterministic laws) then, in principle, a short-term prediction could be possible. The main problems in modelling this type of systems are their complexity and the large dimensionality, which prompts the development of models that are as simple as possible but still account for the main features of the phenomenon.

In this work, we have demonstrated the presence of chaos, estimated the MLE and analysed the bifurcation maps of the two-block BK model for different values of both the characteristic velocity ν_c and the ratio between the strength of the harmonic and leaf springs k. As a final remark, several directions for future investigations can be outlined.

First, it would be interesting to better understand the role of back motion. As mentioned in Section 3.4, the results obtained here are in agreement with the results by de Sousa Vieira [1], where back-slip is not allowed. This last assumption is based on the fact that the relative motion between adjacent tectonic plates occurs in a predominant direction but, as stated by Galvanetto [26], this cannot completely exclude the possibility of occurence of the reverse motion, at least locally and for short time intervals. In the same paper, it is demonstrated that if the static friction is much larger than the kinetic friction then the influence of the no back-slip assumption is more evident. However, there is no obvious need to consider the hypothesis of no backward motion.

Second, to better characterise the system and its dynamics, it might be useful to evaluate the *fractal dimension* of the attractors and the spectrum of Lyapunov exponents. As mentioned in Section 3.4.2, the main problem is that the blocks spend most of the time standing still. Therefore, the dynamics is spike-like, and existing algorithms for the estimation of the Lyapunov spectrum are not capable of fully probing it, at least in their standard form. In addition, one could also extend the bifurcation diagrams to a wider region of parameter space and better characterise the route to chaos.

Finally, a phenomenon that is worth investigating is the so-called synchronized chaos for the three-block model (or any higher dimension model). This may have applications in the field of seismology because, due to the elastic properties of tectonic plates, there could be coupling mechanisms between earthquakes faults that could in principle synchronize. If synchronization happens among elements of a large system, the dimensionality of the attractor decreases and this fact could simplify the analysis, allowing even more detailed models to be used.

Bibliography

[1] Maria de Sousa Vieira. “Chaos and synchronized chaos in an earthquake model”. In: *Physical Review Letters* 82.1 (1999), p. 201.

[2] Edward Lorenz. “The butterfly effect”. In: *World Scientific Series on Nonlinear Science Series A* 39 (2000), pp. 91–94.

[3] Henri Poincaré and Francis Maitland. *Science and method*. Courier Corporation, 2003.

[4] H. Poincaré and B.D. Popp. *The Three-Body Problem and the Equations of Dynamics: Poincaré's Foundational Work on Dynamical Systems Theory*. Astrophysics and Space Science Library. Springer International Publishing, 2017.

[5] E.N. Lorenz. *The Essence Of Chaos*. Jessie and John Danz lectures. Taylor & Francis, 1995. ISBN: 9780295975146.

[6] Edward N Lorenz. “Deterministic nonperiodic flow”. In: *Journal of atmospheric sciences* 20.2 (1963), pp. 130–141.

[7] V. Moretti. *Meccanica analitica. Meccanica classica, meccanica lagrangiana e hamiltoniana e teoria della stabilità*. La matematica per il 3+2. Springer Verlag, 2020. ISBN: 9788847039988.

[8] Julien C Sprott. *Elegant chaos: algebraically simple chaotic flows*. World Scientific, 2010.

[9] R. Devaney. *An Introduction To Chaotic Dynamical Systems*. Studies in Nonlinearity. Avalon Publishing, 2003. ISBN: 9780813340852.

[10] Edward Ott. *Chaos in dynamical systems*. Cambridge university press, 2002.

[11] Benoit B Mandelbrot. “Is nature fractal?” In: *Science* 279.5352 (1998), pp. 783–783.

[12] Celso Grebogi et al. “Strange attractors that are not chaotic”. In: *Physica D: Nonlinear Phenomena* 13.1-2 (1984), pp. 261–268.

[13] Henry DI Abarbanel et al. “The analysis of observed chaotic data in physical systems”. In: *Reviews of modern physics* 65.4 (1993), p. 1331.

[14] Celso Grebogi and James A. Yorke. “The impact of chaos on science and society”. In: 1997.

[15] Helena E. Nusse, James A. Yorke, and Eric J. Kostelich. “Bifurcation Diagrams”. In: *Dynamics: Numerical Explorations: Accompanying Computer Program Dynamics*. New York, NY: Springer US, 1994, pp. 229–268.

[16] Robert M May. “Simple mathematical models with very complicated dynamics”. In: *The Theory of Chaotic Attractors*. Springer, 2004, pp. 85–93.

[17] Valentina Svalova. *Earthquakes: Forecast, Prognosis and Earthquake Resistant Construction*. BoD–Books on Demand, 2018.

[18] Jean M Carlson and JS Langer. “Properties of earthquakes generated by fault dynamics”. In: *Physical Review Letters* 62.22 (1989), p. 2632.

[19] Hiizu Nakanishi. “Complex behavior in earthquake dynamics”. In: *International Journal of Modern Physics B* 12.03 (1998), pp. 273–284.

[20] B. Gutenberg and C. Richter. *Seismicity of the Earth and Associated Phenomena*. Princeton University Press, 1949.

[21] R. Burridge and L. Knopoff. “Model and theoretical seismicity”. In: *Bulletin of the Seismological Society of America* 57.3 (June 1967), pp. 341–371.

[22] Guglielmo Lacorata and Giovanni Paladin. “Predictability time from the seismic signal in an earthquake model”. In: *Journal of Physics A: Mathematical and General* 26.14 (1993), p. 3463.

[23] Stuart Field, Naia Venturi, and Franco Nori. “Marginal stability and chaos in coupled faults modeled by nonlinear circuits”. In: *Physical review letters* 74.1 (1995), p. 74.

[24] S. Boccaletti et al. “The synchronization of chaotic systems”. In: *Physics Reports* 366.1 (2002), pp. 1–101. ISSN: 0370-1573.

[25] Louis M Pecora and Thomas L Carroll. “Synchronization in chaotic systems”. In: *Physical review letters* 64.8 (1990), p. 821.

[26] Ugo Galvanetto. “Some remarks on the two-block symmetric Burridge–Knopoff model”. In: *Physics Letters A* 293.5-6 (2002), pp. 251–259.